Published in final edited form as:
Glia. 2015 February ; 63(2): 313–327. doi:10.1002/glia.22752.

Reactive retinal microglia, neuronal survival and the formation of retinal folds and detachments

Andy J. Fischer[1,*], **Christopher Zelinka**[1], and **Nima Milani-Nejad**[2]

[1]Department of Neuroscience, College of Medicine, The Ohio State University, 4190 Graves Hall, 333 West 10th Ave, Columbus, OH 43210-1239

[2]Department of Physiology and Cell Biology, College of Medicine, The Ohio State University, 370 West 9th Ave, Columbus, OH 43210-1239

Abstract

Reactive microglia and macrophages are prevalent in damaged retinas. Accordingly, we investigate how the activation or ablation of microglia/macrophages influences the survival of neurons in the chick retina *in vivo*. We applied intraocular injections of interleukin 6 (IL6) to stimulate the reactivity of microglia/macrophages and clodronate-liposomes to ablate microglia/macrophages. Activation of the microglia/macrophages with IL6 delays the death of retinal neurons from *N*-methyl-D-aspartate (NMDA) -induced excitotoxicity. In addition, activation of microglia/macrophages combined with colchicine-mediated retinal damage diminished the survival of ganglion cells. Application of IL6 after an excitotoxic insult greatly exacerbates the damage, and causes widespread retinal detachments and folds, accompanied by accumulation of microglia/macrophages in the subretinal space. Damage-induced retinal folds and detachments were significantly reduced by the ablation of microglia/macrophages. We conclude that microglial reactivity is detrimental to the survival of ganglion cells in colchicine-damaged retinas and detrimental to the survival of photoreceptors in retinal folds. In addition, we conclude that IL6-treatment transiently protects amacrine and bipolar cells against an excitotoxic insult. We propose that suppressing reactivity of microglia/macrophages may be an effective means to lessen the damage and vision loss resulting from damage, in particular during retinal detachment injuries.

Keywords

retina; microglia; Müller glia; neuronal survival; retinal detachment

Introduction

Distinct types of glial cells are found within the retina. Common to retinas of all vertebrate species are Müller glia and microglia. With variability between vertebrate species, retinal glia can include astrocytes and oligodendrocytes. A vascular retinas, including those of chickens, guinea pigs and rabbits, contain oligodendrocytes that myelinate the axons of ganglion cells in the nerve fiber layer (NFL). Vascular retinas contain significant numbers of

[*]corresponding author: Andy J. Fischer, Department of Neuroscience, Ohio State University, College of Medicine, 3020 Graves Hall, 333 W. 10th Ave, Columbus, OH 43210-1239, USA. Telephone: (614) 292-3524; Fax: (614) 688-8742; Andrew.Fischer@osumc.edu.

astrocytes, that are closely associated with the blood vessels (Schnitzer 1987; Schnitzer 1988). By comparison, the retinas of guinea pigs and birds do not contain conventional types of astrocytes (Fischer and Bongini 2010; Fischer et al. 2010a; Fujita et al. 2001; Won et al. 2000). The chick retina, but not guinea pig retina, contains an atypical glial cell, termed Non-astrocytic Inner Retinal Glia-like (NIRG) cells, that is scattered across inner retinal layer (Fischer et al. 2010a; Fischer et al. 2010b).

Glial activity can have a significant impact upon neuronal survival. For example, conditional ablation of the Müller glia compromises photoreceptor survival and vascular integrity in the rodent retina (Shen et al. 2012). Glial cells can profoundly exacerbate neuronal death following excitotoxic injury. For example, *N*-methyl-D-aspartate (NMDA) -mediated activity of Müller glia is known to activate the NFκB-pathway and stimulate tumor necrosis factor α (TNFα) production by the Müller glia, and the TNFα influences the Ca^{2+} -permeability of AMPA-receptors in retinal neurons to diminish survival (Lebrun-Julien et al. 2009). Similarly, intraocular injections of insulin stimulate the reactivity of Müller glia, microglia and NIRG cells, and predispose retinal neurons to excitotoxic damage (Fischer et al. 2009a). Conversely, stimulation of glia can provide enhanced neuroprotection. For example, we found that the neuroprotective effects of fibroblast growth factor 2 (FGF2) are manifested through activation of Mitogen-Activated Protein Kinase (MAPK) -signaling in the Müller glia (Fischer et al. 2009a). Similar to the Müller glia, microglia have been implicated in the pathophysiology of different sight-threatening diseases. Microglia were thought to be bystanders cells that do not contribute to retinal degeneration. However, current consensus indicates that activated microglia and/or infiltrating macrophages contribute to the progression of age-related macular degeneration, glaucoma and diabetic retinopathy (reviewed by Buschini et al. 2011; Karlstetter et al. 2010; Langmann 2007; Xu et al. 2009). Taken together, these findings suggest that the activity of retinal glia is coordinated and can have a significant influence upon neuronal survival and the progression of retinal degeneration.

Cytokines can have a significant effect upon glial reactivity and neuronal survival. In IL6-deficient mice, compared to wild-type mice, acute injury results in significantly reduced reactivity in Glial Fibriliary Acidic Protein (GFAP) -positive astrocytes and microglia (Klein et al. 1997). In GFAP-IL6-overexpressing transgenic mice, astrocytes produce elevated levels of IL6 which results in lifelong reactive gliosis of both astrocytes and microglia (Chiang et al. 1994). In response to brain trauma resulting from a cryo-lesion, neuronal damage was reduced and recovery was accelerated in the GFAP-IL6 mice compared to the injury response seen in wild-type mice, suggesting a neuroprotective role for elevated IL6 in neural tissues (Penkowa et al. 2003). A recent study demonstrated that murine Müller glia exposed to activated microglia have altered cell morphology and gene expression compared to Müller glia undergoing gliosis (Wang et al. 2011). Activated microglia may influence Müller glia directly, and exchange pro-inflammatory and chemotactic cytokines that mediate adaptive glial activity in the retina in response to injury (Wang et al. 2011). We recently found that reactive microglia and/or macrophages stimulate the formation of Müller glia-derived progenitors in the chick retina (Fischer et al. 2014). The current study investigates how activation or ablation of microglia and/or macrophages influences neuronal survival

and retinal folds/detachments in acutely damaged chick retinas *in vivo*. The chick retina is an ideal model system in which to examine the depletion of microglia/macrophages because the efficacy of depletion approaches 100% and this depletion is sustained for at least 4 weeks (Zelinka et al. 2012).

Methods and Materials

Animals

The use of animals in these experiments was in accordance with the guidelines established by the National Institutes of Health and The Ohio State University. This study was approved by the Ohio State University Institutional Animal Care and Use Committee (IACUC). Newly hatched leghorn chickens (*Gallus gallus domesticus*) were obtained from the Department of Animal Sciences at the Ohio State University and kept on a cycle of 12 hours light, 12 hours dark (lights on at 7:00 am). Chicks were housed in a stainless steel brooder at about 25°C and received water and Purina™ chick starter *ad libitum*.

Preparation of clodronate-liposomes

The preparation of clodronate liposomes was based on previous descriptions (Van Rooijen 1989; van Rooijen 1992; Van Rooijen and Sanders 1994). The protocols used to generate clodronate liposome were as described previously (Zelinka et al. 2012). Approximately 1% of the clodronate is encapsulated by the lipsomes (Van Rooijen and Sanders 1994), yielding approximately 7.85 mg/ml. Precise quantitation of the clodronate was difficult, because of the stochastic nature of combination of the clodronate and liposomes. Accordingly, we titered-down doses of clodronate liposomes to levels where >99% of the microglia/macrophages were ablated at 1 day after treatment.

Intraocular injections

Chickens were anesthetized via inhalation of 2.5% isoflurane in oxygen and intraocular injections performed as described previously (Fischer et al., 1998; Fischer et al., 1999; Fischer et al., 1999). For all experiments, the left eyes of chicks were injected with the “test” compound and the contra-lateral right eyes were injected with vehicle as a control. Compounds were injected in 20 μl sterile saline with 0.05 mg/ml bovine serum albumin added as a carrier. Compounds used in these studies included Interleukin-6 (100 or 200ng/dose), NMDA (38.5 or 154 μg/dose), colchicine (200 ng/dose), and clodronate liposomes (10 to 2000 ng). Two μg of BrdU was injected to label proliferating cells. Injection paradigms are included in each figure.

Tissue dissection, fixation, sectioning and immunolabeling

Tissues were fixed, sectioned and immunolabeled as described elsewhere (Fischer et al. 1998; Fischer and Stell 1999). Retinal whole-mount preparations were processed as described previously (Fischer et al. 2008; Fischer et al. 2006). Working dilutions and sources of antibodies used in this study included; (1) mouse anti-CD45 was used at 1:200 (HIS-C7; Cedi Diagnostic), (2) mouse anti-PCNA was used at 1:1000 (MO879; Dako Immunochemicals), (3) mouse anti-Brn3a (Pouf4a) was used at 1:50 (mab1585; Chemicon), (4) rabbit anti-Sox9 was used at 1:2000 (AB5535; Chemicon), and (5) mouse (IgG) anti-

transitin was used at 1:50 (EAP3; DSHB). None of the observed labeling was due to non-specific binding of secondary antibody or autofluorescence because sections labeled with secondary antibodies alone were devoid of fluorescence. Secondary antibodies included donkey-anti-goat-Alexa488/568, goat-anti-rabbit-Alexa488/568/647, goat-anti-mouse-Alexa488/568/647, and goat-anti-rat-Alexa488 (Invitrogen) diluted to 1:1000 in PBS plus 0.2% Triton X-100. Some sections were counter-stained with the nuclear label DRAQ5 (Cell Signaling) diluted to 1:2000 and added to the secondary antibody diluent.

Labeling microglia with RCA1

Ricinus communis agglutinin-1 (RCA1) is a well-established marker for microglia/macrophages in the avian central nervous system (Cuadros et al. 2006). The protocol for labeling with biotinylated RCA1 has been described in detail in a previous report (Fischer et al. 2010a).

Terminal deoxynucleotidyl transferase dUTP nick end labeling (TUNEL)

To identify dying cells that contained fragmented DNA the TUNEL method was used. We used an *In Situ* Cell Death Kit (TMR red; Roche Applied Science), as per the manufacturer's instructions.

Microscopy and quantitative immunofluorescence

Wide-field photomicrographs were obtained by using a Leica DM5000B microscope and Leica DC500 digital camera. Images were optimized for brightness and contrast, multiple-channel images overlaid, and figures constructed by using Adobe Photoshop™6.0. Cell counts were made from at least 5 different animals, and means and standard deviations calculated on data sets. To avoid the possibility of region-specific differences within the retina, cell counts were consistently made from the same region of retina for each data set.

Similar to previous reports (Fischer et al. 2009a; Fischer et al. 2009b; Fischer et al. 2010a), immunofluorescence was quantified by using ImagePro 6.2 (Media Cybernetics, Bethesda, MD, USA). Identical illumination, microscope, and camera settings were used to obtain images for quantification. Retinal areas were sampled from 5.4 MP digital images. These areas were randomly sampled over the inner nuclear layer (INL) where the nuclei of the bipolar and amacrine neurons were observed. Measurements were made for regions containing pixels with intensity values of 68 or greater (0 = black and 255 = saturated); a threshold that included labeling in the bipolar or amacrine neurons. The total area was calculated for regions with pixel intensities > 68. The average pixel intensity was calculated for all pixels within threshold regions. The density sum was calculated as the total of pixel values for all pixels within threshold regions. These calculations were determined for retinal regions sampled from six different retinas for each experimental condition.

Percentage area of retinal folds and detachments was determined from digital micrographs. The detached areas appeared as opacities that were digitally traced and measured by using ImagePro 6.2. The detached retinal area was calculated as a percentage of total retinal area without compensating for concave shape of the eyecup.

Cell counts and statistics

Where significance of difference was determined between two treatment groups accounting for inter-individual variability (means of treated-control values) we performed a two-tailed, paired t-test. Where significance of difference was determined between two treatment groups we performed a two-tailed, unpaired t-test. Levene's test was used to test for unequal variances. For data sets with unequal variances, we performed a Kruskal-Wallis non-parametric ANOVA.

Results

IL6 and reactive microglia/macrophages influence the survival of retinal neurons

We began by examined whether intraocular injections of IL6 prior to NMDA-treatment influenced the survival of retinal neurons and the reactivity of microglia. We have recently reported that intraocular injections of IL6 stimulate the reactivity of microglia, increase retinal levels of pro-inflammatory cytokines, IL1β and TNFα, and increase levels of p38 MAPK in Müller glia in the absence of damage (Fischer et al. 2014). At one day after NMDA-treatment, when numbers of TUNEL-positive cells are known to be maximal (Fischer et al. 1998), pre-treatment with IL6 significantly reduced numbers of dying cells by about 75% (Figs. 1a–c). It is possible that IL6-mediated activation of microglia resulted in a rapid clearance of dying cells, and reduced numbers of TUNEL-positive cells at 24 hours after NMDA-treatment. However, at 4 hrs after NMDA-treatment we observed fewer TUNEL-positive cells in retinas pretreated with IL6 (data not shown). To examine whether cell death was delayed in IL6/NMDA-treated retinas we probed for cell death at 3 days after NMDA-treatment when most of the cell death is known to subside (Fischer et al. 1998). We found that numbers of TUNEL-positive cells were significantly increased, by nearly 5-fold, in the INL at 3 days after NMDA-treatment in retinas that were pretreated with IL6 (Figs. 1d–f). At 3 days after NMDA-treatment, we frequently observed folds or focal retinal detachments in control and treated retinas (Fig. 1g). These retinal folds contained numerous dying photoreceptors in the ONL and interneurons in the INL (Fig. 1h,j). The abundance of TUNEL-positive cells was far greater in folded regions compared to regions of retina that remained adherent to the retinal pigmented epithelium (RPE; Figs. 1h–j).

To examine the reactivity of microglia we probed for CD45 and RCA1, and assessed amoeboid morphology. The CD45- and RCA1-labeling does not distinguish between retinal microglia and infiltrating macrophages. Thus, for simplicity, hereafter, we will use the term "microglia/macrophage" to collectively refer to retinal microglia and infiltrating macrophages. One day after NMDA-treatment, we observed significant increases (240.2 ± 36.0%; n=6; $p<0.0001$) in the number of CD45+ cells in retinas that were pretreated with IL6 (Figs. 2a and 2b). In IL6/NMDA-treated retinas, many of the microglia/macrophages were PCNA-positive (Figs. 2c–e), suggesting that local proliferation underlies the IL6-mediated accumulation of CD45+ microglia/macrophages. At 3 days after NMDA-treatment when the abundance and reactivity of microglia/macrophages are known to be maximal (Fischer et al. 1998; Zelinka et al. 2012), there were no obvious differences in the abundance and reactivity of microglia/macrophages (Figs. 2f and g). Many of the microglia/macrophages in the IPL were positive for PCNA (Figs. 2h–n), suggesting that the

accumulation resulted, at least in part, from local proliferation. At or near regions of retinal folds we frequently observed putative macrophages adherent to the vitread surface of the retina that were intensely labeled for RCA1 (Fig. 2o).

We next examined whether IL6-treatment prior to colchicine-treatment influences ganglion cell survival. When injected during the early post-hatch period, colchicine is known to destroy numerous ganglion cells (Fischer et al. 1999; Fischer et al. 2008; Morgan 1981). We found that IL6-treatment significantly reduced the numbers of surviving Brn3a-positive ganglion cells in central and temporal regions of the retina, whereas numbers of surviving cells were unaffected in dorsal and nasal regions of the retina (Figs. 3a–c). The loss of ganglion cells in dorsal and nasal was nearly complete, thereby not permitting a determination of the survival-diminishing effects of IL6. The damaging effects of colchicine upon ganglion cells are rapidly diminished with increasing age (Fischer et al. 1999; Morgan 1981). Therefore, we tested whether IL6-treatment influenced the survival of ganglion cells under conditions of reduced damage with increased treatment age (Fig. 3d). We found that IL6-treatment had no significant effect upon ganglion cell survival in all regions of the retina when the colchicine was applied at P5 (Fig. 3d–f).

We next examined whether the survival-reducing effects of insulin and the survival-promoting effects of IL6 were mediated through the microglia/macrophages. We ablated the microglia/macrophages with clodronate-liposomes, injected insulin and then damaged retinal neurons with NMDA. We have previously reported that clodronate-liposomes are phagocytized by IL6-activated microglia at the inner limiting membrane (ILM), and the vast majority (>90%) of microglia perish within 24 hours of treatment (Zelinka et al., 2012). We have recently reported that intraocular injections of insulin or IGF1 stimulate the reactivity of microglia and render retinal neurons more susceptible to NMDA-induced excitotoxicity (Fischer et al. 2009a; Fischer et al. 2010a). Consistent with a previous report (Fischer et al. 2009a), injection of insulin before NMDA increased the abundance of reactive microglia/macrophages and NIRG cells in the IPL (Figs. 4a,b,d,e) and doubled the number of TUNEL-positive cells in the INL (Fig. 4j). When a single dose of IL6 was applied 5 days before NMDA, there was not a significant decrease in the number of TUNEL-positive cells (Fig. 4j). However, the survival-diminishing effects of insulin are completely overridden by pre-treatment with IL6 (Fig. 4j). When the microglia/macrophages were ablated with IL6 and clodronate-liposomes, we found significantly fewer dying cells in NMDA-damaged retinas (Fig. 4j). Interestingly, the ability of IL6 to override the survival-diminishing effects of insulin is lost when the microglia/macrophages were ablated by clodronate-liposomes (Figs. 4b,c,h–j).

Reactive microglia/macrophages influence focal retinal detachments and folds

We found that retinal folds and detachments that occurred following different damage paradigms, involving different dose regimens of NMDA and IL6, were completely prevented by the ablation of microglia/macrophages. In response to a high dose (2 μmol) NMDA, we found that nearly 15% of the retinal area was folded/detached, and this area was reduced by 94% in retinas when the microglia/macrophages were ablated (Figs. 5a and b). By comparison, a lower dose (0.5 μmol) of NMDA resulted in relatively few retinal folds/

detachments (Figs. 5c and d). However, when IL6 was applied after the lower dose of NMDA we found numerous wide-spread folds/detachments that increased the area of folded/detached retina by more than 6-fold compared to that of controls (Figs. 5c and d). To test whether the IL6-induced retinal folds/detachments were caused by reactive monocytes, we ablated the microglia/macrophages before the NMDA/IL6-treatment (Fig. 5e). In retinas where IL6 was applied 3 days before the NMDA/IL6-treatment there was significantly ($p=0.00012$) less area that was folded/detached compared to retinas where NMDA-treatment was followed by IL6 (6.0 ± 1.4% vs 17.3 ± 3.3%; Figs. 5d and f). Nevertheless, the ablation of the microglia/macrophages completely prevented the folds that resulted from NMDA/IL6-treatment (Figs. 5e and f).

We performed cell death and immunohistochemical analyses to better understand the changes in NMDA-damaged retinas where the microglia/macrophages were activated or ablated. In control retinas treated with IL6 before a 2 μmol-dose of NMDA there were numerous, reactive microglia/macrophages concentrated within the IPL (Fig. 6a), similar to previous descriptions (Fischer et al. 1998; Zelinka et al. 2012). By comparison there was a complete absence of microglia/macrophages in NMDA-damaged retinas pre-treated with IL6/clodronate (Fig. 6b). The loss of microglia was complete across all regions of the retina, similar to a previous report (Zelinka et al. 2012). In folded/detached regions of control retina, we always observed reactive microglia/macrophages in the subretinal space and in some instances the accumulation of microglia/macrophages in the subretinal space of the fold was enormous (Fig. 6c). Consistent with previous reports (Zelinka et al. 2012), there was an accumulation of Sox9-positive NIRG cells in regions of the IPL of NMDA-damaged retinas that remained adherent to the RPE (Fig. 6d). By comparison, few NIRG cells were observed in retinas treated with IL6/clodronate before NMDA (Fig. 6e). The death of NIRG cells in IL6/clodronate-treated retinas is believed to be secondary to the loss of microglia (Zelinka et al. 2012). In folded/detached regions of retina reactive Müller glia were prevalent (Fig. 6f).

In regions of retina that remained adherent to the RPE, the ablation of the microglia/macrophages before NMDA-treatment significantly increased numbers of TUNEL-positive cells compare to NMDA-damaged retinas that contained reactive microglia/macrophages (Figs. 6g–j). Most of the TUNEL-positive cells in non-detached regions of retina were found in the amacrine cell layer of the INL, and dying cells were not observed in the ONL (Figs. 6g and h). By comparison, in detached regions of control retinas we found numerous TUNEL-positive cells in the ONL (Fig. 6i).

To examine the effects of IL6-stimulated microglia/macrophages on stressed retinas, 3 consecutive daily doses of IL6 were applied following a lower dose (500 nmol) of NMDA. IL6-mediated stimulation of microglia/macrophages greatly exacerbated the retinal damage cause by NMDA. The enhanced damage observed in retinas treated with IL6 after NMDA was manifested as extensive detachments and folds (Figs. 7a–c). The detached portions of the retina ranged from single folds, that were about 400 μm deep (Figs. 7b,f,i and l), to convoluted detachments that extended more than 1 mm away from the RPE (Fig. 7c). Sox9-expressing Müller glia appeared reactive, or transitioning into a progenitor-like phenotype, in both treated and control retinas with elevated levels of transitin and some delamination of

nuclei away from the center of the INL (Figs. 7d and e). Müller glia were present in regions of retinal folds and detachments (Fig. 7f), unlike in the folds that result from IGF1/NMDA-treatment (Fischer et al. 2010a). By comparison, there were few NIRG cells (Sox9+Nkx2.2) observed in adherent or detached regions of retinas treated with NMDA/IL6 (not shown). Although IL6 stimulates the reactivity of microglia/macrophage, these cells did not appear to be more reactive or abundant in adherent regions of retinas treated with NMDA/IL6 compared to those seen in retinas treated with NMDA/saline (Figs. 7g and h). In eyes treated with NMDA/IL6, regions of detached retina contained numerous CD45-positive microglia/macrophages within the subretinal space (Fig. 7i).

In regions of retina that remained attached to the RPE we observed significantly fewer TUNEL-positive cells in retinas treated with IL6 after NMDA compared to controls (Figs. 7j–m). Most of the dying cells were found in the amacrine cell layer of INL in adherent regions of retina (Figs. 7j and k). In treated retinas, TUNEL-positive cells were most abundant in detached regions and most of these dying cells were in the ONL (Fig. 7l), but dying cells were also observed in the INL in larger detachments (see Fig 8j for an example). The presence of TUNEL-positive cells in the ONL suggested that photoreceptors were perishing in retinas treated with IL6 after NMDA.

We next examined the retinas where the microglia/macrophages were ablated and then treated with a 500 nmol dose of NMDA followed by intravitreal injections of IL6. There were accumulations of Sox9-positive NIRG cells in the IPL of retinas treated with NMDA/IL6, whereas there were few Sox9-positive NIRG cells in retinas treated with IL6-clodronate/NMDA/IL6 (Figs. 8a–c). In eyes treated with IL6 alone before a 500 nmol dose of NMDA/IL6, non-detached regions of retina contained numerous reactive microglia/macrophages that were concentrated with the IPL (Fig. 8e). In detached/folded regions of the retina, we observed accumulations of microglia/macrophages in the subretinal space (Fig. 8f). By comparison, in eyes treated with IL6+clodronate before a NMDA/IL6 there was a complete absence of microglia/macrophages across all regions of the retina (Fig. 8g). In non-detached regions of the retina numbers of TUNEL-positive cells were nearly three-fold more abundant when the microglia/macrophages were ablated (Figs. 8h,i and k). Not surprisingly, there were numerous TUNEL-positive cells in the outer layers of retina in regions of detachments/folds (Fig. 8j).

Discussion

We find that intraocular injections of IL6 and reactive microglia/macrophages can have profound effects upon neuronal survival and retinal detachment (RD). We find that intraocular injections of IL6 transiently protect retinal neurons against an excitotoxic insult, whereas IL6 can diminish the survival of stressed ganglion cells. When IL6 was applied after a relatively modest excitotoxic insult, widespread retinal folds and death of photoreceptors were induced. Since NMDA is not known to directly damage photoreceptors and there were dying photoreceptor cells in the ONL in regions of retina that remained attached to the RPE, the loss of photoreceptors in folded regions of NMDA-damaged retinas is secondary to the excitotoxicity. We consistently find accumulations of microglia/macrophages in the subretinal space of folds and detachments that result from different

damage paradigms and IL6-dosing regimens. When the microglia/macrophages were ablated, retinal folds and detachments were almost completely prevented, regardless of types of damage- and cytokine-treatments, and the death of photoreceptors was obviated.

RD is a prevalent cause of vision loss in humans. The pathobiology of RD involves changes to the photoreceptors, Müller glia and microglia/macrophages. Common to different animal models of RD is the degeneration of photoreceptor outer segments and subsequent death of many photoreceptor cells (Chang et al. 1995; Cook et al. 1995). In addition, Müller glia are known to proliferate and become reactive, with up-regulation of intermediate filaments (Fisher and Lewis 2003; Lewis et al. 2003; Sethi et al. 2005). Consistent with our findings in the chick model system, many studies in mammalian model systems have demonstrated that macrophages and microglia become reactive, accumulate in the retina and subretinal space, and may contribute to retinal pathology following RD (Kaneko et al. 2008; Lewis et al. 2005; Nakazawa et al. 2007). Here we provide evidence that reactive microglia/macrophages are detrimental to RD and the ablation of the microglia is beneficial to prevent or protect against RD. In retinas where the microglia/macrophages were ablated, retinal folds and detachments did not form and dying photoreceptor cells were absent. We have recently characterized the chick model of saline and hyalurinoic acid-induced RDs, and demonstrated local photoreceptor degeneration and death, microglial reactivity and Müller glial reactivity (Cebulla et al. 2012), similar to the cellular responses in mammalian models of RD (reviewed by Fisher and Lewis 2003; Fisher et al. 2005; Lewis et al. 2002). We find numerous reactive Müller glia in the damaged retinas, within adherent and detached regions of the retina, and the Müller glia remained reactive even when the microglia/macrophages were ablated. Collectively, our data indicate that reactive Müller glia do not cause retinal folds and detachments in retinas treated with NMDA and/or IL6. It remains uncertain whether the infiltration of microglia/macrophages into the subretinal space soon after an insult initiates the formation of detachments, or whether the arrival of microglia/macrophages into the subretinal after an initial focal detachment exacerbates the damage and prevents reattachment of the retina. Nevertheless, we conclude that the fold/detachment-inhibiting effects of IL6/clodronate-liposomes are mediated by the absence of reactive retinal microglia/macrophages.

We find that IL6-mediated activation of microglia/macrophages before NMDA dramatically, but transiently, reduces numbers of dying neurons. The NMDA-insult was induced at 1 day after IL6-treatment when retinal levels of ADAM17 and TNFα are known to be reduced (Fischer et al. 2014). In addition, we find that IL6-treatment before an excitotoxic insult increased the reactive phenotype of the microglia/macrophages and increased the proliferation of these cells. We find that treatment with IL6 before colchicine attenuated the survival of ganglion cells. Colchicine-induced death of ganglion cells peaks at about 3–4 days after treatment (Fischer et al. 1999), when retinal levels of ADAM17 and TNFα are elevated by IL6-treatment (Fischer et al. 2014). Retinal levels of proinflammatory cytokines, such as IL1β and TNFα, likely mediate glial reactivity and neuronal survival. For example, TNFα is known to be expressed at elevated levels by “activated” Müller glia (Lebrun-Julien et al. 2009), and p38 MAPK is known to be upstream of TNFα biosynthesis (Aberg et al. 2006). Thus, IL6-mediated activation of microglia/macrophages may secondarily influence Müller glial reactivity and synthesis of TNFα. The survival-

influencing effects of IL6 may vary between cell types and may be time-dependent. Thus, it will be critical to identify the affected cell types and time-course of IL6-mediated effects if IL6-signaling is to be used as a therapeutic target. These findings are consistent with the hypothesis that the production of TNFα by Müller glia may regulate IL6-mediated neuronal survival/death.

The activation of microglia and macrophages within the nervous system can be detrimental to neuronal survival. For example, there is significant evidence that inflammation and microglial reactivity negatively influence the neuronal degeneration that occurs within Parikinson's disease (reviewed by Tansey and Goldberg 2010). Similarly, persistent neurological deficits and chronic neurodegeneration that occur with the demyelinating autoimmune disease Multiple Sclerosis appear to result from activated microglia and invading macrophages (reviewed by Kierdorf et al. 2010). It is well established that with increasing age there is increased microglial reactivity, and this increase in the inflammatory profile of the microglia has negative behavioral and cognitive consequences (reviewed by Norden and Godbout 2013). Thus, there is significant evidence that microglial reactivity can significantly influence neuronal function and survival. In the eye, a recent study has demonstrated that the survival of retinal ganglion cells is compromised and correlated with activated microglia when rats are immunized by retinal homogenates (Joachim et al. 2012). This finding suggests that over-activation of retinal microglia/macrophages can be detrimental to the survival of retinal neurons.

Within non-detached regions of NMDA-damaged retinas the ablation of microglia/macrophages may have been detrimental to neuronal survival. We found increased numbers of dying cells in adherent regions of retina at 3 days after NMDA-treatment when the microglia/macrophages were ablated. It is possible that the loss of microglia/macrophages in clodronate-treated retinas results in increased delayed cell death. Alternatively, the loss of phagocytic microglia/macrophages may have resulted in increased numbers of TUNEL-positive cells because the dying cells were not cleared from the retina. Along these lines of reasoning, it is possible that few TUNEL-positive cells were seen in IL6-treated/NMDA-damaged retinas because the dead cells were cleared faster by the IL6-stimulated microglia/macrophages. However, even at 4 hours after NMDA-treatment the IL6-pretreated retinas contained fewer dying cells, indicating that hyperactivation of microglia/macrophages did not accelerate the clearance of cells from damaged retinas. Another distinct possibility is that the IL6-activated microglia go through different activation states that occur at different time-points after damage (Boche et al. 2013; Kierdorf et al. 2010; Wong 2013). Changes in activation states of the microglia might explain the transient neuroprotective effects of IL6 that occur shortly after damage and subsequently shift toward survival diminishing effects. Nevertheless, the molecular mechanisms underlying the transient neuroprotective effects of IL6 in excitotoxin-damaged retinas remain uncertain.

We found that a single dose of IL6 three days before NMDA/IL6-treatment reduced the mean area of folded/detached retina compared to NMDA/IL6-treated retinas without the IL6-pretreatment. It is possible that IL6-primed microglia/macrophages do not further over-react in damaged retinas with additional exposure to IL6. Alternatively it is possible that pretreatment with IL6 desensitizes the responses of microglia/macrophages to damage

combined with additional exposure to IL6. Microglia/macrophages are known to respond rapidly to an intravitreal delivery of IL6. For example, an intravitreal delivery of IL6 causes the rapid evacuation of microglia/macrophages from within the retina, and migration and accumulation to the vitread surface (Zelinka et al. 2012).

Conclusions

We conclude that reactive microglia/macrophages can have profound effects upon neuronal survival in damaged retinas. Our data indicate that reactive microglia/macrophages exacerbate NMDA-induced retinal damage, in part by stimulating the accumulation of microglia/macrophages in the subretinal space. The ablation of the microglia/macrophages prevents the formation of folds and detachments in damaged retinas, whereas IL6-treatment greatly enhances the formation of folds and detachments in damaged retinas. Collectively, our findings suggest that reactive microglia/macrophages are detrimental to retinal folds and detachments. Further, the neuroprotective effects of IL6 can override the survival-diminishing effects of insulin in NMDA-damaged retinas. Our findings suggest that ablation of microglia/macrophage, suppression of microglial reactivity, or drawing microglia/macrophages away from the photoreceptors might be viable strategies to minimize the damaged incurred by retinal detachment.

Acknowledgments

We thank Donika Gallina, Levi Todd, and Dr. Colleen M. Cebulla for comments that contributed to the final form of this paper. The transitin (developed by Dr. G. Cole) antibody was obtained from the Developmental Studies Hybridoma Bank developed under auspices of the NICHD and maintained by the University of Iowa, Department of Biological Sciences, Iowa City, IA 52242. This work was supported by a grant (EY022030-02) from the National Institutes of Health.

References

Aberg ND, Brywe KG, Isgaard J. Aspects of growth hormone and insulin-like growth factor-I related to neuroprotection, regeneration, and functional plasticity in the adult brain. Scientific World Journal. 2006; 6:53–80. [PubMed: 16432628]

Boche D, Perry VH, Nicoll JA. Review: activation patterns of microglia and their identification in the human brain. Neuropathol Appl Neurobiol. 2013; 39(1):3–18. [PubMed: 23252647]

Buschini E, Piras A, Nuzzi R, Vercelli A. Age related macular degeneration and drusen: neuroinflammation in the retina. Prog Neurobiol. 2011; 95(1):14–25. [PubMed: 21740956]

Cebulla CM, Zelinka CP, Scott MA, Lubow M, Bingham A, Rasiah S, Mahmoud AM, Fischer AJ. A chick model of retinal detachment: cone rich and novel. PLoS One. 2012; 7(9):e44257. [PubMed: 22970190]

Chang CJ, Lai WW, Edward DP, Tso MO. Apoptotic photoreceptor cell death after traumatic retinal detachment in humans. Arch Ophthalmol. 1995; 113(7):880–6. [PubMed: 7605279]

Chiang CS, Stalder A, Samimi A, Campbell IL. Reactive gliosis as a consequence of interleukin-6 expression in the brain: studies in transgenic mice. Dev Neurosci. 1994; 16(3–4):212–21. [PubMed: 7535683]

Cook B, Lewis GP, Fisher SK, Adler R. Apoptotic photoreceptor degeneration in experimental retinal detachment. Invest Ophthalmol Vis Sci. 1995; 36(6):990–6. [PubMed: 7730033]

Cuadros MA, Santos AM, Martin-Oliva D, Calvente R, Tassi M, Marin-Teva JL, Navascues J. Specific immunolabeling of brain macrophages and microglial cells in the developing and mature chick central nervous system. J Histochem Cytochem. 2006; 54(6):727–38. [PubMed: 16461367]

Fischer AJ, Bongini R. Turning Muller glia into neural progenitors in the retina. Mol Neurobiol. 2010; 42(3):199–209. [PubMed: 21088932]

Fischer AJ, Morgan IG, Stell WK. Colchicine causes excessive ocular growth and myopia in chicks. Vision Res. 1999; 39(4):685–97. [PubMed: 10341956]

Fischer AJ, Ritchey ER, Scott MA, Wynne A. Bullwhip neurons in the retina regulate the size and shape of the eye. Dev Biol. 2008; 317(1):196–212. [PubMed: 18358467]

Fischer AJ, Scott MA, Ritchey ER, Sherwood P. Mitogen-activated protein kinase-signaling regulates the ability of Müller glia to proliferate and protect retinal neurons against excitotoxicity. Glia. 2009a; 57(14):1538–1552. [PubMed: 19306360]

Fischer AJ, Scott MA, Tuten W. Mitogen-activated protein kinase-signaling stimulates Muller glia to proliferate in acutely damaged chicken retina. Glia. 2009b; 57(2):166–81. [PubMed: 18709648]

Fischer AJ, Scott MA, Zelinka C, Sherwood P. A novel type of glial cell in the retina is stimulated by insulin-like growth factor 1 and may exacerbate damage to neurons and Muller glia. Glia. 2010a; 58(6):633–49. [PubMed: 19941335]

Fischer AJ, Seltner RL, Poon J, Stell WK. Immunocytochemical characterization of quisqualic acid- and N-methyl-D-aspartate-induced excitotoxicity in the retina of chicks. J Comp Neurol. 1998; 393(1):1–15. [PubMed: 9520096]

Fischer AJ, Skorupa D, Schonberg DL, Walton NA. Characterization of glucagon-expressing neurons in the chicken retina. J Comp Neurol. 2006; 496(4):479–94. [PubMed: 16572462]

Fischer AJ, Zelinka C, Gallina D, Scott MA, Todd L. Reactive microglia and macrophage facilitate the formation of Muller glia-derived retinal progenitors. Glia. 2014 in press.

Fischer AJ, Zelinka C, Scott MA. Heterogeneity of glia in the retina and optic nerve of birds and mammals. PLoS One. 2010b; 5(6):e10774. [PubMed: 20567503]

Fisher SK, Lewis GP. Muller cell and neuronal remodeling in retinal detachment and reattachment and their potential consequences for visual recovery: a review and reconsideration of recent data. Vision Res. 2003; 43(8):887–97. [PubMed: 12668058]

Fisher SK, Lewis GP, Linberg KA, Verardo MR. Cellular remodeling in mammalian retina: results from studies of experimental retinal detachment. Prog Retin Eye Res. 2005; 24(3):395–431. [PubMed: 15708835]

Fujita Y, Imagawa T, Uehara M. Fine structure of the retino-optic nerve junction in the chicken. Tissue Cell. 2001; 33(2):129–34. [PubMed: 11392664]

Joachim SC, Gramlich OW, Laspas P, Schmid H, Beck S, von Pein HD, Dick HB, Pfeiffer N, Grus FH. Retinal ganglion cell loss is accompanied by antibody depositions and increased levels of microglia after immunization with retinal antigens. PLoS One. 2012; 7(7):e40616. [PubMed: 22848388]

Kaneko H, Nishiguchi KM, Nakamura M, Kachi S, Terasaki H. Characteristics of bone marrow-derived microglia in the normal and injured retina. Invest Ophthalmol Vis Sci. 2008; 49(9):4162–8. [PubMed: 18487364]

Karlstetter M, Ebert S, Langmann T. Microglia in the healthy and degenerating retina: insights from novel mouse models. Immunobiology. 2010; 215(9–10):685–91. [PubMed: 20573418]

Kierdorf K, Wang Y, Neumann H. Immune-mediated CNS damage. Results Probl Cell Differ. 2010; 51:173–96. [PubMed: 19130024]

Klein MA, Moller JC, Jones LL, Bluethmann H, Kreutzberg GW, Raivich G. Impaired neuroglial activation in interleukin-6 deficient mice. Glia. 1997; 19(3):227–33. [PubMed: 9063729]

Langmann T. Microglia activation in retinal degeneration. J Leukoc Biol. 2007; 81(6):1345–51. [PubMed: 17405851]

Lebrun-Julien F, Duplan L, Pernet V, Osswald I, Sapieha P, Bourgeois P, Dickson K, Bowie D, Barker PA, Di Polo A. Excitotoxic death of retinal neurons in vivo occurs via a non-cell-autonomous mechanism. J Neurosci. 2009; 29(17):5536–45. [PubMed: 19403821]

Lewis GP, Charteris DG, Sethi CS, Fisher SK. Animal models of retinal detachment and reattachment: identifying cellular events that may affect visual recovery. Eye (Lond). 2002; 16(4):375–87. [PubMed: 12101444]

Lewis GP, Sethi CS, Carter KM, Charteris DG, Fisher SK. Microglial cell activation following retinal detachment: a comparison between species. Mol Vis. 2005; 11:491–500. [PubMed: 16052164]

Lewis HD, Perez Revuelta BI, Nadin A, Neduvelil JG, Harrison T, Pollack SJ, Shearman MS. Catalytic site-directed gamma-secretase complex inhibitors do not discriminate pharmacologically between Notch S3 and beta-APP cleavages. Biochemistry. 2003; 42(24):7580–6. [PubMed: 12809514]

Morgan IG. Intraocular colchicine selectively destroys immature ganglion cells in chicken retina. Neurosci Lett. 1981; 24(3):255–60. [PubMed: 6168980]

Nakazawa T, Hisatomi T, Nakazawa C, Noda K, Maruyama K, She H, Matsubara A, Miyahara S, Nakao S, Yin Y, et al. Monocyte chemoattractant protein 1 mediates retinal detachment-induced photoreceptor apoptosis. Proc Natl Acad Sci U S A. 2007; 104(7):2425–30. [PubMed: 17284607]

Norden DM, Godbout JP. Review: microglia of the aged brain: primed to be activated and resistant to regulation. Neuropathol Appl Neurobiol. 2013; 39(1):19–34. [PubMed: 23039106]

Penkowa M, Giralt M, Lago N, Camats J, Carrasco J, Hernandez J, Molinero A, Campbell IL, Hidalgo J. Astrocyte-targeted expression of IL-6 protects the CNS against a focal brain injury. Exp Neurol. 2003; 181(2):130–48. [PubMed: 12781987]

Schnitzer J. Retinal astrocytes: their restriction to vascularized parts of the mammalian retina. Neurosci Lett. 1987; 78(1):29–34. [PubMed: 3614770]

Schnitzer J. Astrocytes in the guinea pig, horse, and monkey retina: their occurrence coincides with the presence of blood vessels. Glia. 1988; 1(1):74–89. [PubMed: 2976740]

Sethi CS, Lewis GP, Fisher SK, Leitner WP, Mann DL, Luthert PJ, Charteris DG. Glial remodeling and neural plasticity in human retinal detachment with proliferative vitreoretinopathy. Invest Ophthalmol Vis Sci. 2005; 46(1):329–42. [PubMed: 15623793]

Shen W, Fruttiger M, Zhu L, Chung SH, Barnett NL, Kirk JK, Lee S, Coorey NJ, Killingsworth M, Sherman LS, et al. Conditional Muller cell ablation causes independent neuronal and vascular pathologies in a novel transgenic model. J Neurosci. 2012; 32(45):15715–27. [PubMed: 23136411]

Tansey MG, Goldberg MS. Neuroinflammation in Parkinson's disease: its role in neuronal death and implications for therapeutic intervention. Neurobiol Dis. 2010; 37(3):510–8. [PubMed: 19913097]

Van Rooijen N. The liposome-mediated macrophage 'suicide' technique. J Immunol Methods. 1989; 124(1):1–6. [PubMed: 2530286]

van Rooijen N. Liposome-mediated elimination of macrophages. Res Immunol. 1992; 143(2):215–9. [PubMed: 1533469]

Van Rooijen N, Sanders A. Liposome mediated depletion of macrophages: mechanism of action, preparation of liposomes and applications. J Immunol Methods. 1994; 174(1–2):83–93. [PubMed: 8083541]

Wang M, Ma W, Zhao L, Fariss RN, Wong WT. Adaptive Muller cell responses to microglial activation mediate neuroprotection and coordinate inflammation in the retina. J Neuroinflammation. 2011; 8:173. [PubMed: 22152278]

Won MH, Kang TC, Cho SS. Glial cells in the bird retina: immunochemical detection. Microsc Res Tech. 2000; 50(2):151–60. [PubMed: 10891879]

Wong WT. Microglial aging in the healthy CNS: phenotypes, drivers, and rejuvenation. Front Cell Neurosci. 2013; 7:22. [PubMed: 23493481]

Xu H, Chen M, Forrester JV. Para-inflammation in the aging retina. Prog Retin Eye Res. 2009; 28(5): 348–68. [PubMed: 19560552]

Zelinka CP, Scott MA, Volkov L, Fischer AJ. The Reactivity, Distribution and Abundance of Non-Astrocytic Inner Retinal Glial (NIRG) Cells Are Regulated by Microglia, Acute Damage, and IGF1. PLoS One. 2012; 7(9):e44477. [PubMed: 22973454]

Main Points

- Reactive microglia/macrophages accumulate in the subretinal space of detached/folded regions of retina.
- Activation of microglial reactivity with a pro-inflammatory cytokine exacerbates retinal folds and detachments
- Ablation of reactive microglia/macrophages in the retina completely prevents the formation of folds and detachments

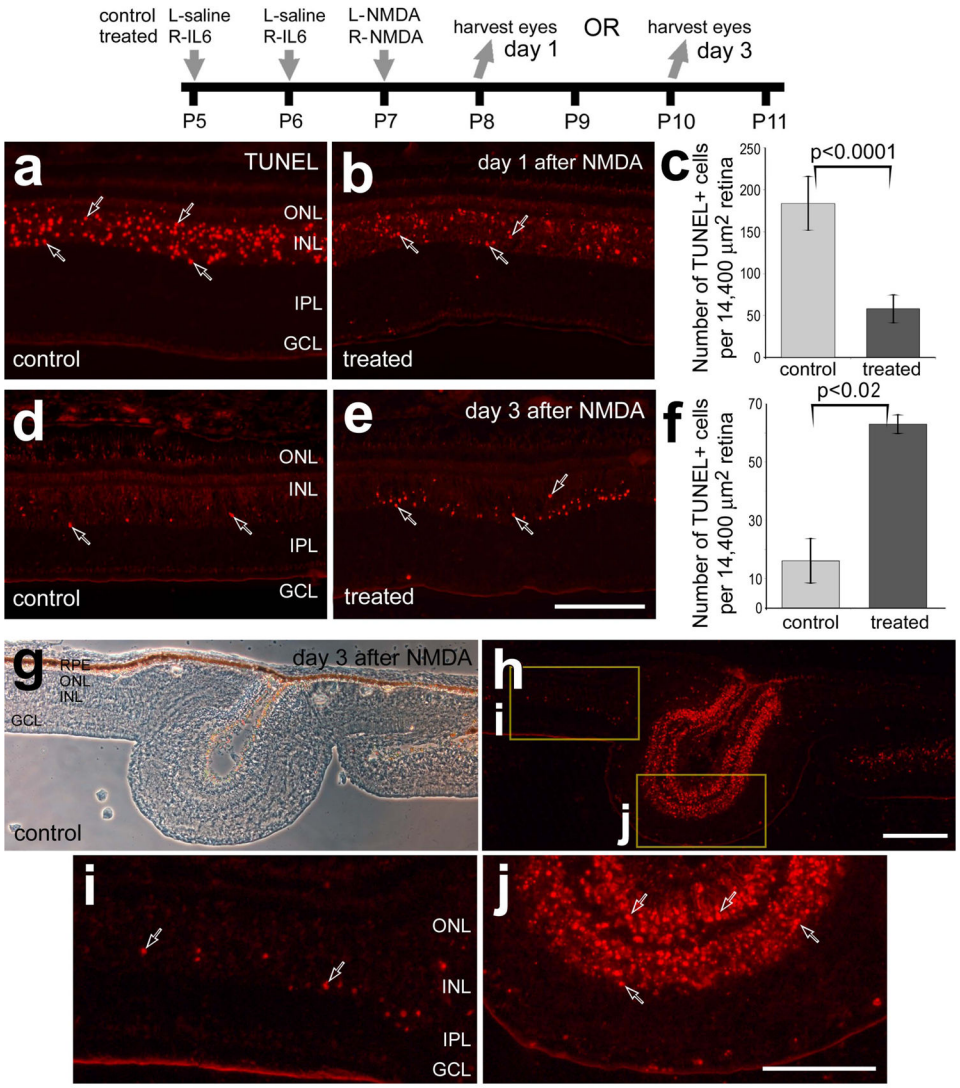

Figure 1.

IL6 delays cell death in NMDA-damaged retinas. Retinas were obtained from eyes that were injected with IL6 (or saline) at P5 and P6, NMDA at P7, and harvested at P8 (1 day after NMDA; **a**–**c**) or at P10 (3 days after NMDA; **d**–**j**). Vertical sections of the retina were fluorescently labeled *in situ* for fragmented DNA (TUNEL; **a**,**b**,**d**,**e** and **h**–**j**) or images were taken using phase contrast imaging (**g**). Hollow arrows indicate TUNEL-positive nuclei. The boxed areas in panel **h** are enlarged 3.5-fold in panels **i** and **j**. Panels **c** and **f** are histograms illustrating the mean (±SD) number of TUNEL-positive nuclei per 14,400 µm^2 in retinas treated with saline/NMDA or IL6/NMDA. Significance (*p<0.02, **p<0.0001) of difference between control and treated groups was determined using a two-tailed, unpaired t-test. The scale bar (50 µm) in panel **e** applies to **a, b, d** and **e**, the bar in **g** applies to **g** and **h,** and the bar in **j** applies to **j** and **i**. Abbreviations: ONL – outer nuclear layer, INL – inner nuclear layer, IPL – inner plexiform layer, GCL – ganglion cell layer, RPE- retinal pigmented epithelium.

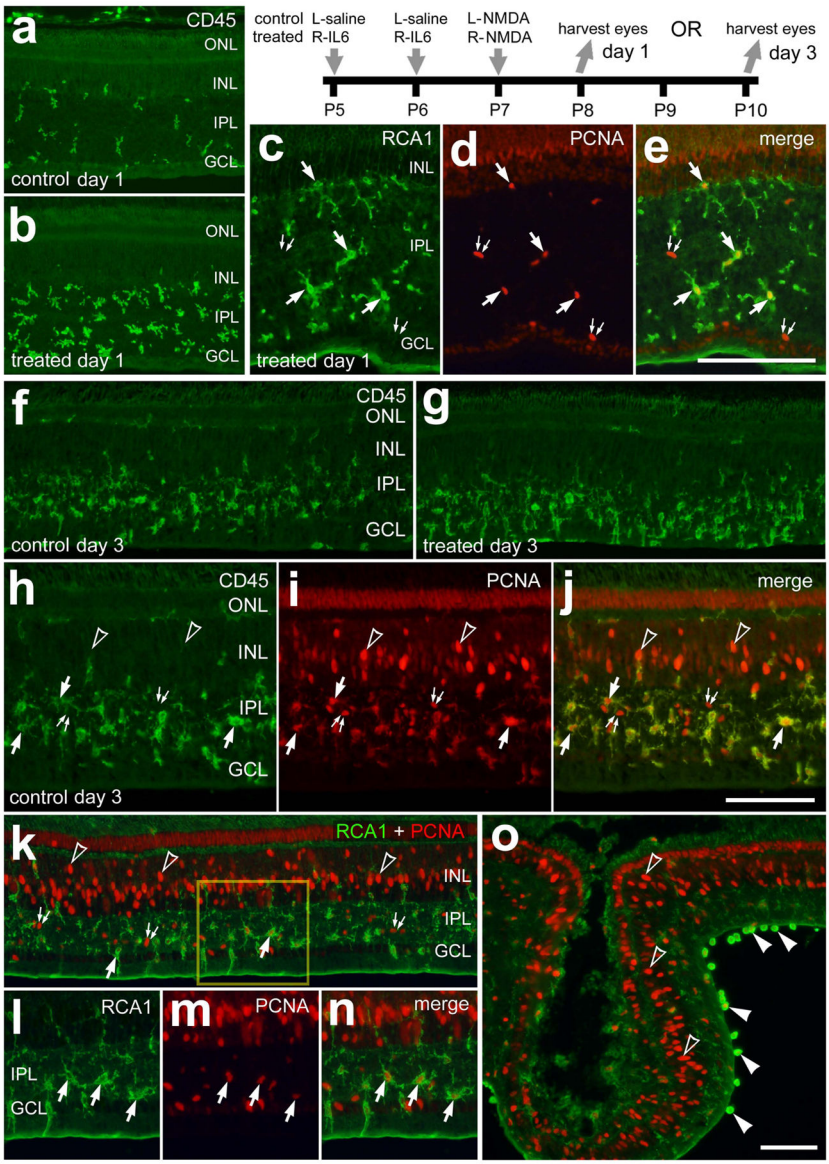

Figure 2.

IL6-treatment accelerates the accumulation of reactive microglia and marcrophage in NMDA-damaged retinas. Retinas were obtained from eyes that were injected with IL6 (or saline) at P5 and P6, NMDA at P7, and harvested at P8 (1 day after NMDA; **a**–**e**) or P10 (3 days after NMDA; **h**–**o**). Vertical sections of the retina were labeled with RCA1 (green; **c**, **e**, **k**, **l**, **n** and **o**), antibodies to CD45 (green; **a**, **b**, **f**–**h** and **j**) or antibodies to PCNA (red; **d**, **e**, **i**–**k** and **m**–**o**). The arrows indicate microglia/macrophage, small double-arrows indicate NIRG cells, hollow arrow-heads indicate the nuclei of Müller glia, and solid arrow-heads indicate presumptive macrophages at the vitread surface of the retina. The scale bar (50 μm) in panel **c** applies to **c**–**e**, the bar **j** applies to **h**–**j** and the bar in **o** applies to **a**, **b**, **f**, **g**, **k** and **o**. The boxed-out area in **k** is enlarged 2-fold in **l**–**n**. Abbreviations: ONL – outer nuclear layer, INL – inner nuclear layer, IPL – inner plexiform layer, GCL – ganglion cell layer, PCNA – proliferating cell nuclear antigen.

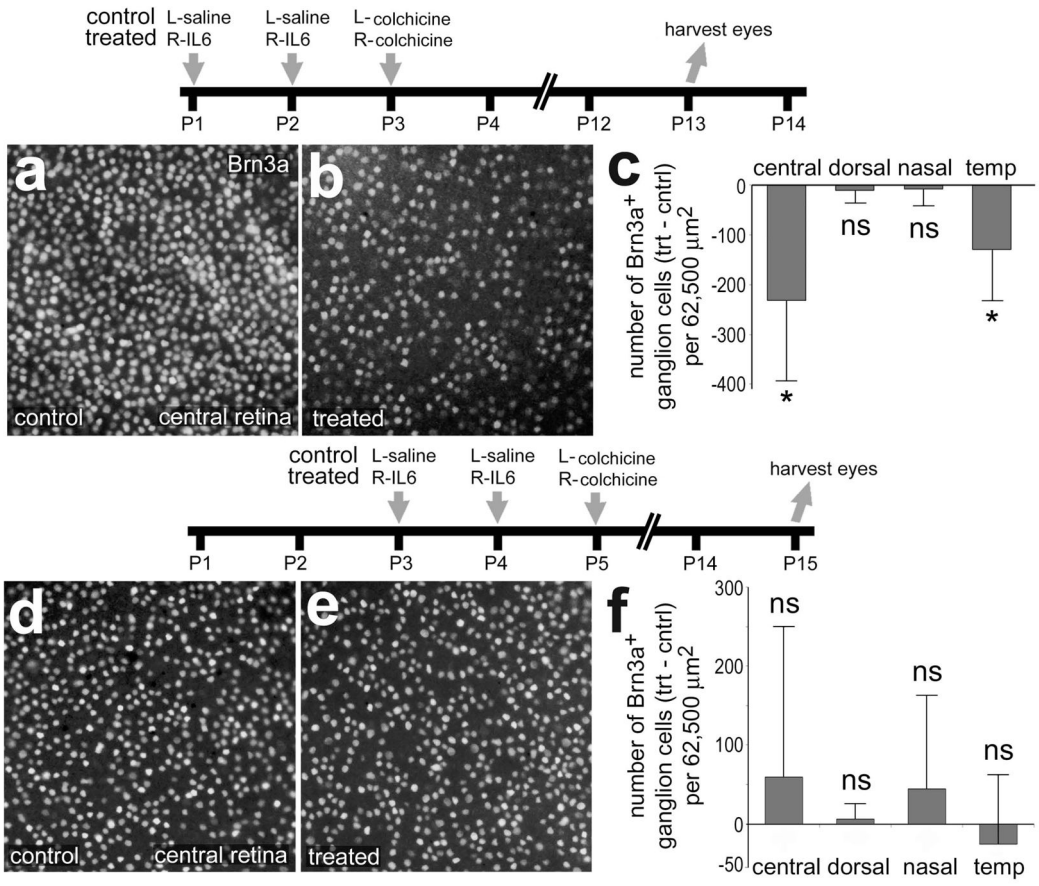

Figure 3.

IL6 renders ganglion cells more susceptible to damage and this effect is transient during the course of early post-hatch development. Retinas were obtained from eyes that were injected with IL6 (or saline) at P1 and P2, colchicine at P3 and harvested at P13 (**a**–**c**). Retinas were injected IL6 alone (control) or IL6+clodronate (treated) at P1, IL6 at P3 and P4, colchicine at P5, and harvested at P15 (**d**–**e**). Whole-mount preparations of central regions of the retina were labeled with antibodies to Brn3a (**a**, **b**, **d** and **e**). Histograms in **c** and **f** illustrate the mean (±SD) number of Brn3a-positive ganglion cells in central, dorsal, nasal and temporal regions of the retina. Significance (*$p<0.05$, ns $p>0.05$) of difference between treated-control groups for each region of retinas was determined using a two-tailed, paired t-test.

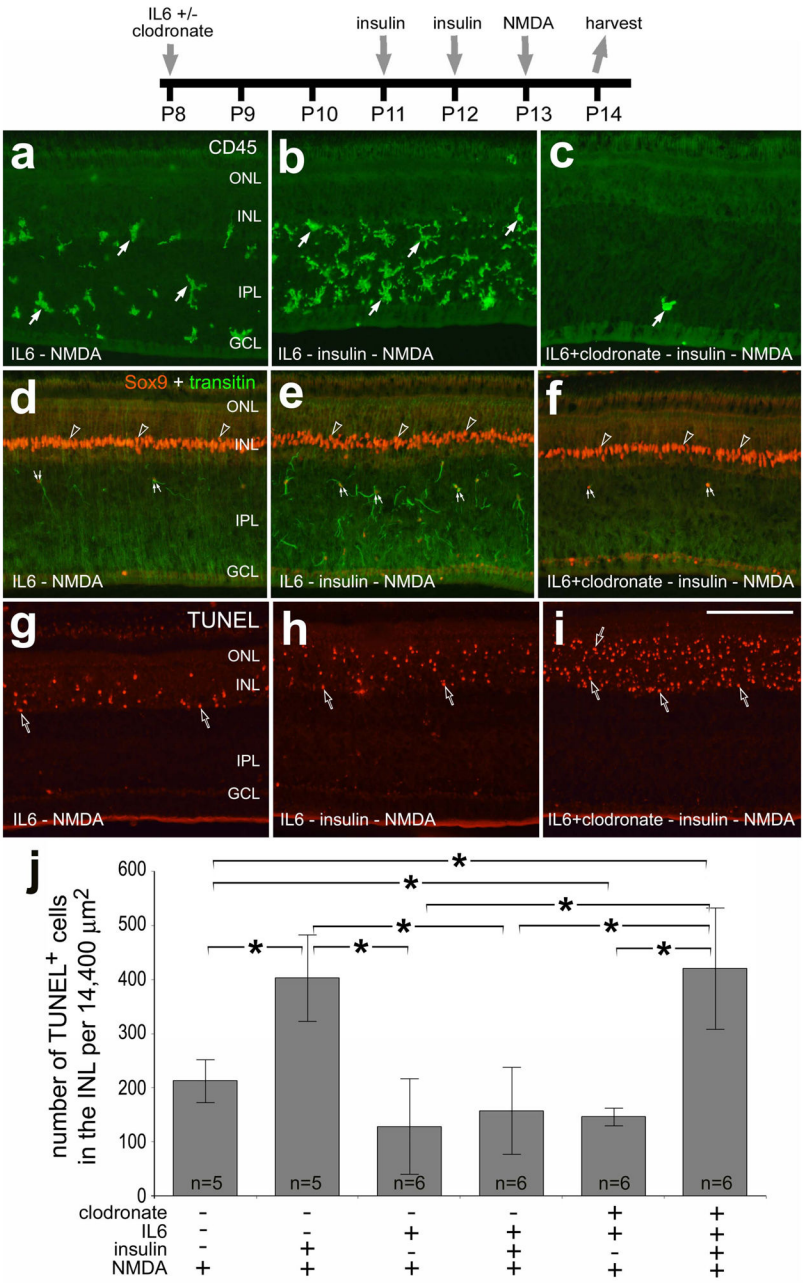

Figure 4.

The survival-diminishing effects of insulin in NMDA-damaged retinas are not elicited through the activation of microglia/macrophages and/or NIRG cells. Retinas were obtained from eyes injected with combinations of IL6, clodronate-liposomes, insulin and NMDA. Vertical sections of the retina were labeled with antibodies to CD45 (**a**–**c**), Sox9 (red) and transitin (green; **d**–**f**), or the TUNEL method (**g**–**i**). The arrows indicate microglia/macrophage, small double-arrows indicate NIRG cells, and hollow arrow-heads indicate the nuclei of Müller glia. The scale bar (50 µm) in panel **i** applies to **a**–**i**. The histogram in **j** illustrates the mean (±SD) number of TUNEL-positive cells in the INL (14,400 μm^2). A Levene's test indicated unequal variances among the comparison groups. Therefore, we

performed a non-parametric Kruskal-Wallis ANOVA ($p<0.0002$). Significance of difference (*$p<0.05$) indicates no overlap of 95% confidence intervals. Abbreviations: ONL – outer nuclear layer, INL – inner nuclear layer, IPL – inner plexiform layer, GCL – ganglion cell layer.

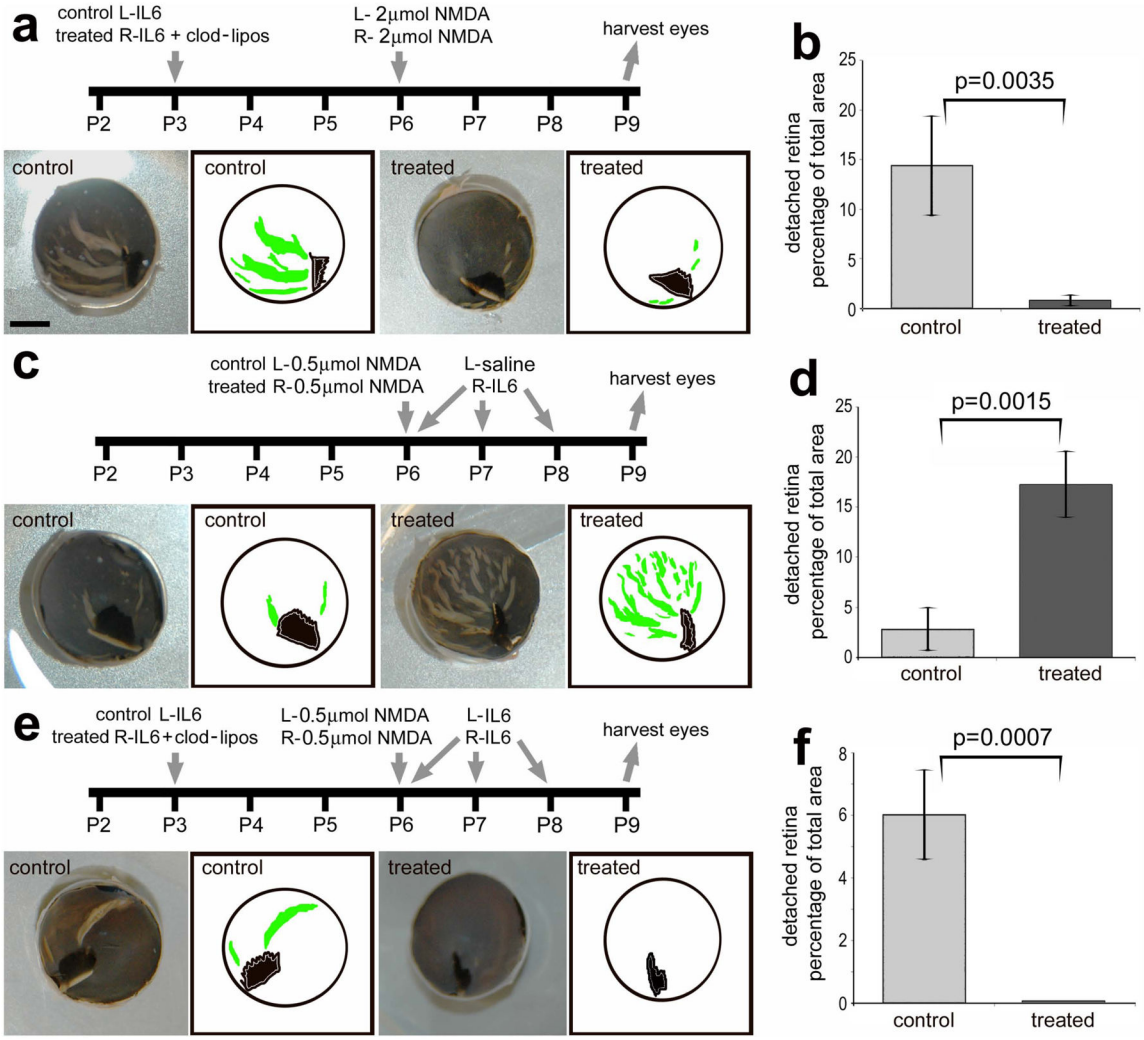

Figure 5.

Activation of microglia/macrophages with IL6 increases retinal detachments and folds, whereas the ablation of microglia/macrophages prevents the formation of retinal detachments and folds. Experimental paradigms for injections of IL6, clodronate-liposomes and NMDA are outlined for each data set (**a**, **c** and **e**). Images include digital photographs and digital tracings of the eyecup circumference (black), pecten (black) and retinal folds/detachments (green; **a**, **c** and **e**). The scale bar (5 mm) in panel **a** applies to **a**, **c** and **e**. The histograms in panels **b**, **d** and **f** illustrate the mean (± SD) percentage of retinal area that is detached/folded in the different experimental paradigms. The significance of difference (*p<0.005, **p<0.0001) was determined by using a two-tailed, unpaired t-test. Percentage area of retinal folds and detachments was determined from digital micrographs. The detached areas appeared as opacities that were digitally traced and measured by using ImagePro 6.2. The detached retinal area was calculated as a percentage of total retinal area without compensating for concave shape of the eyecup.

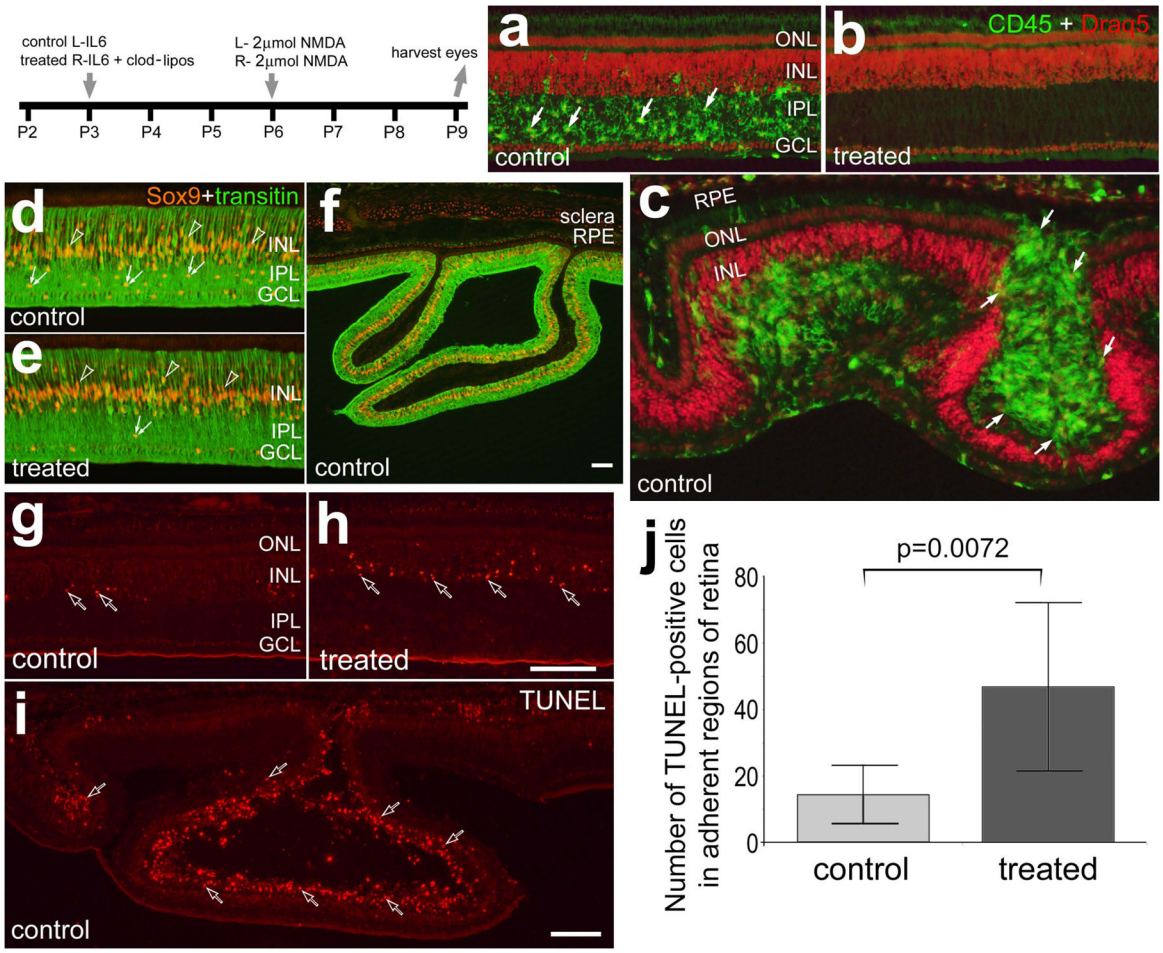

Figure 6.

Reactive microglia and/or macrophages accumulate in the subretinal space of NMDA-induced retinal folds and detachments which are prevented by the ablation of retinal microglia/macrophages. Beginning at P3, control eyes were injected with IL6 alone and treated eyes were injected with IL6 and clodronate-liposomes. Eyes were injected with 2 µmol of NMDA at P6 and harvested 3 days later at P9. Retinas were labeled for CD45 (green) and Draq5 (red; **a**–**c**), Sox9 (red) and transitin (green; **d**–**f**), or dying cells identified with the TUNEL method (**g**–**i**). Arrows indicate microglia/macrophage, hollow arrows indicate dying cells, small double-arrows indicate the nuclei of NIRG cells, and hollow arrow-heads indicate the nuclei of Müller glia. The scale bar (50 µm) in panel **h** applies to **a**–**e, g** and **h**, the bar in **f** applies to **f** alone, and the bar in **i** applies to **i** alone. The histogram in **j** illustrates the mean (± SD) of TUNEL positive cells per 6600 μm^2 retina. Cell counts were made only within central regions of retina that remained adherent to the RPE. The significance of difference (p-value) was determined by using a two-tailed, unpaired t-test. Abbreviations: ONL – outer nuclear layer, INL – inner nuclear layer, IPL – inner plexiform layer, GCL – ganglion cell layer.

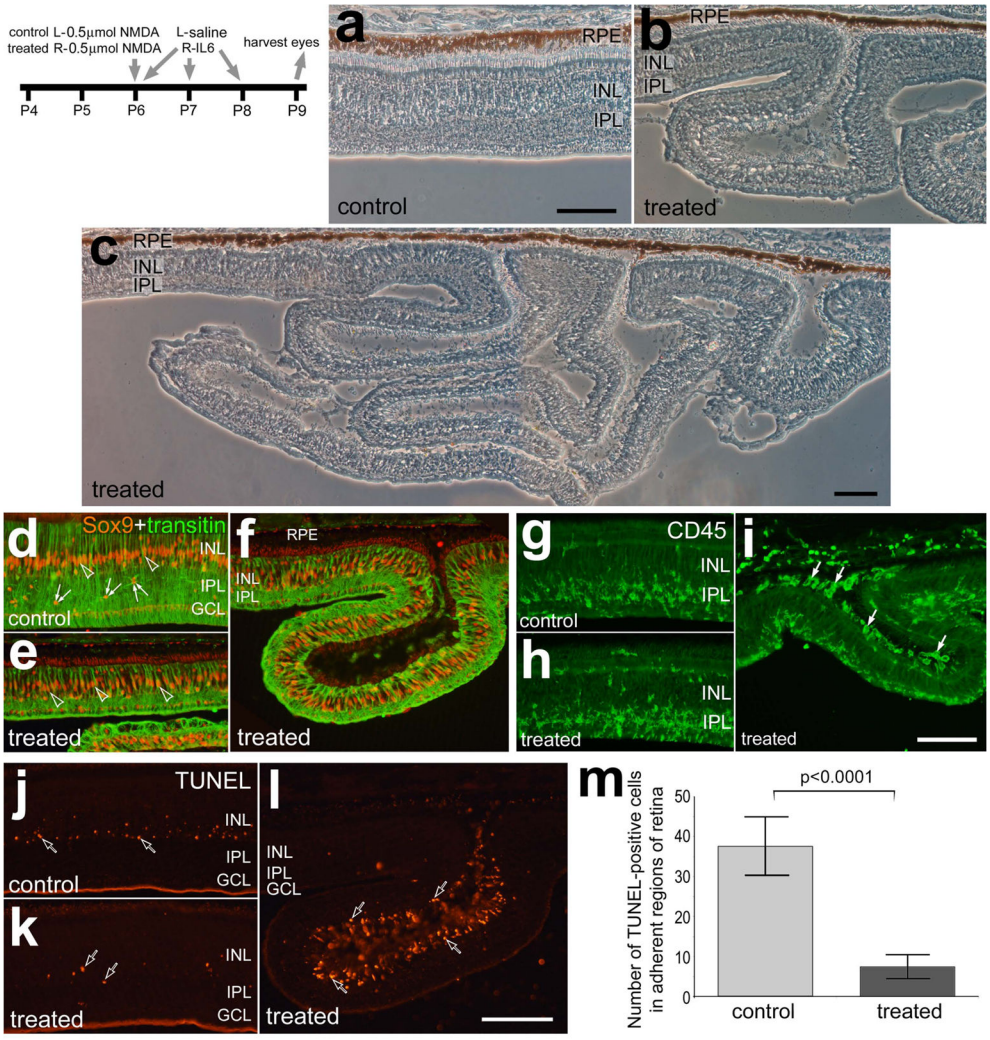

Figure 7.

IL6-mediated stimulation of microglia/macrophages after NMDA-induced damage results in widespread retinal folds and detachments and accumulations of reactive microglia/macrophages in the subretinal space. Eyes were injected with 0.5 µmol of NMDA at P6. Control eyes were injected with saline and treated eyes were injected with 200ng IL6 at 4 hrs, 24 hrs and 48 hrs after the NMDA-treatment. Eyes were harvested at P9. The micrographs in **a**, **b** and **c** are phase contrast images of control and treated retinas. Retinas were labeled for Sox9 (red) and transitin (green; **d**–**f**), CD45 (**g**–**i**), or dying cells were labeled with the TUNEL method (**j**– **l**). Arrows indicate microglia/macrophage, hollow arrows indicate dying cells, small double-arrows indicate the nuclei of NIRG cells, and hollow arrow-heads indicate the nuclei of Müller glia. The scale bar (50 µm) in panel **a** applies to **a** and **b**, the bar in **c** applies **c** alone, the bar in **i** applies to **d**–**i**, and the bar in **l** applies to **j**–**l**. The histogram in **m** illustrates the mean (± SD) of TUNEL positive cells per 6600 μm^2 retina. Cell counts were made only within central regions of retina that remained adherent to the RPE. The significance of difference (p-value) was determined by using a two-tailed, unpaired t-test. Abbreviations: RPE – retinal pigmented epithelium, ONL – outer

nuclear layer, INL – inner nuclear layer, IPL- inner plexiform layer, GCL – ganglion cell layer.

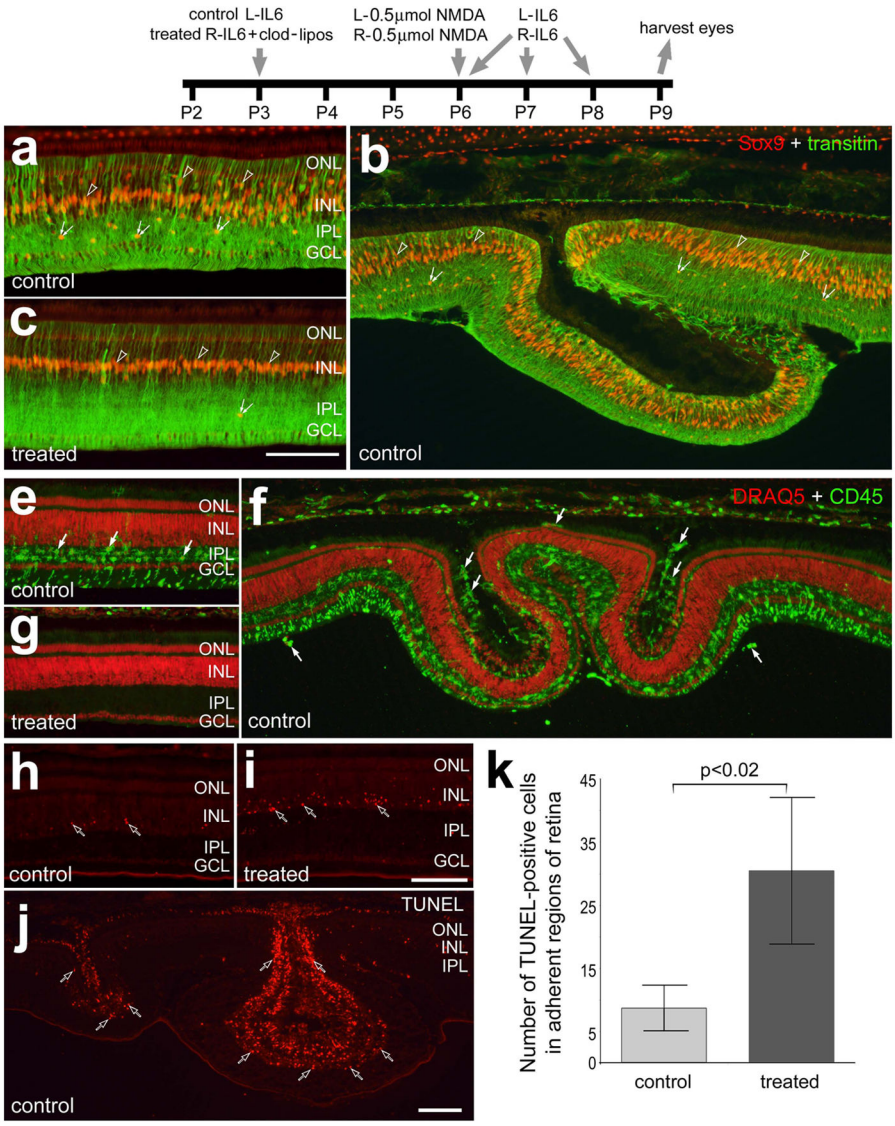

Figure 8.

IL6-induced retinal folds in NMDA-damaged retinas are prevented by the ablation of retinal microglia/macrophages. Beginning at P3, control eyes were injected with IL6 alone and treated eyes were injected with IL6 and clodronate-liposomes. Eyes were injected with 0.5 µmol of NMDA at P6. Control eyes were injected with saline and treated eyes were injected with 200ng IL6 at 4 hrs, 24 hrs and 48 hrs after the NMDA-treatment. Eyes were harvested at P9. Retinas were labeled for Sox9 (red) and transitin (green; **a**–**c**), CD45 (green) and Draq5 (red; **e**–**g**), or dying cells with the TUNEL method (**h**–**j**). Arrows indicate microglia/macrophage, hollow arrows indicate dying cells, small double-arrows indicate the nuclei of NIRG cells, and hollow arrow-heads indicate the nuclei of Müller glia. The scale bar (50 µm) in panel **c** applies to **a**–**c**, and the bar in **j** applies to **e**–**j**. The histogram in **k** illustrates the mean (± SD) of TUNEL positive cells per 6600 μm^2 retina. The significance of difference (p-value) was determined by using a two-tailed, unpaired t-test. Cell counts were made only within central regions of retina that remained adherent to the RPE.

Abbreviations: ONL – outer nuclear layer, INL – inner nuclear layer, IPL – inner plexiform layer, GCL – ganglion cell layer.